Rare Metal Materials and Engineering
Volume 49, Issue 10, October 2020
Available online at www.rmme.ac.cn

Science Press

Cite this article as: Rare Metal Materials and Engineering, 2020, 49(10): 3353-3360.

ARTICLE

Investigation on Creep Behavior of Zr-based Bulk Metallic Glass by Nanoindentation

Li Chunyan[1,2], Zhu Fuping[1], Ding Juanqiang[1], Yin Jinfeng[1], Wang Zheng[3], Zhao Yanchun[1,2], Kou Shengzhong[1,2]

[1] State Key Laboratory of Advanced Processing and Reuse of Nonferrous Metals, Lanzhou University of Technology, Lanzhou 730050, China; [2] Wenzhou Engineering Institute of Pump & Valve, Lanzhou University of Technology, Wenzhou 325105, China; [3] Sinotruk Group Jinan Truck Company Limited, Jinan 250000, China

Abstract: The effect of loading rate and holding time on the creep deformation behavior of $(Zr_{0.6336}Cu_{0.1452}Ni_{0.1012}Al_{0.12})_{97.4}Er_{2.6}$ bulk metallic glass (BMG) was investigated by nanoindentation technique. Results demonstrate that the creep displacement of the specimen increases with the increase of loading rate or holding time. On the other hand, the hardness (H) of specimen falls with the rise of loading rate or holding time. The H drops with the growth of indentation depth during the nanoindentation process, which indicates that the specimen has a size effect. The specimen shows a serrated flow phenomenon which has rate dependence. Specifically, as the loading rate declines, the serrated flow phenomenon becomes more obvious. The creep stress exponent of the specimen goes down with the increases of loading rate or holding time.

Key words: nanoindentation; hardness; loading rate; stress exponent; holding time

In recent years, due to the characteristics such as high hardness and strength, superior wear resistance and excellent corrosion resistance, bulk metallic glass (BMG) has received extensive attention from the whole world scholars[1-6]. However, the limited size and room temperature brittleness of BMG are two key bottlenecks which currently hinder the application in structural materials[7,8]. Although scientists have a keen interest in the excellent mechanical properties of BMG, the deformation mechanisms are still not fully understood due to their limited plasticity[9]. The development of nanoindentation technique has effectively improved the understanding of the deformation behavior of BMG. Compared with the traditional macro-performance test methods, the nanoindentation method has significant features. Nanoindentation technique has high resolution in terms of the recording for data of load-displacement. Nanoindentation technique has been widely used to characterize the mechanical response of BMG, such as the time-dependent behavior (i.e., creep)[10-19]. Moreover, nanoindentation technique has significant advantages in the study of mechanical properties and deformation of materials in small size. It is well known that the creep behavior of crystalline materials is mainly performed by dislocation slip, atomic diffusion, etc. However, the creep mechanism of BMG is still unknown. According to Refs[20,21], whether BMG has low or high glass transition temperature (T_g), all BMGs exhibit creep deformation at room temperature. Nanoindentation technique can be used to study the creep behavior of BMG at room temperature accurately.

In the present work, the effect of loading rate and holding time on creep behavior of $(Zr_{0.6336}Cu_{0.1452}Ni_{0.1012}Al_{0.12})_{97.4}Er_{2.6}$ BMG were studied. In addition, the creep deformation process and mechanism of BMG was analyzed.

1 Experiment

Master alloy with nominal composition of $(Zr_{0.6336}Cu_{0.1452}$-

Received date: October 12, 2019
Foundation item: National Natural Science Foundation of China (51661016, 51861021, 51571105, 51661017); Wenzhou Public Welfare Science and Technology Project (G20170019)
Corresponding author: Li Chunyan, Ph. D., Professor, School of Materials Science and Engineering, Lanzhou University of Technology, Lanzhou 730050, P. R. China, Tel: 0086-931-2976378, E-mail: licywz@163.com

$Ni_{0.1012}Al_{0.12})_{97.4}Er_{2.6}$ was chosen in this study, due to its excellent glass forming ability (GFA), superior thermal stability and outstanding plasticity at room temperature. The master alloy was fabricated by levitation melting the constituent elements Zr (99.95%), Cu (99.98%), Ni (99.98%), Al (99.98%) and Er (99.99%) under a high purity argon atmosphere. Master alloy was re-melted three times to ensure chemical homogeneity, followed by suction casting into a water-cooled copper mold in order to get rods with a diameter of 3 mm and a length of 70 mm. The structures of specimens were investigated by X-ray diffractometer (XRD, D/max-2400, Cu Kα). The thermal characteristic temperatures of specimen were evaluated by differential scanning calorimeter (DSC, STA449C) with a heating rate of 20 K/min. Energy dispersive spectrometer (EDS) was used to quantitatively analyze the components of specimen.

Test specimen for nanoindentation investigation, with a diameter of 3 mm and a length of 3 mm, was polished to mirror smooth finish. Nanoindentation investigation was carried out by using Hysitron Ti 950 Triboindenter with a standard Berkovich diamond indenter at room temperature. Experiments were performed at diverse loading rates of 500, 1000, 1500 and 2000 μN/s with a load limit of 10 000 μN and a holding period of 10 s. The load was unloaded to zero at the same rate finally. In order to study the effect of holding time on the nano-mechanical properties of specimen, various holding time were selected, such as 5, 10, 15 and 20 s, and the uniform loading rate was 500 μN/s. The indentation morphology was observed by a scanning probe microscope (SPM).

2 Results and Discussion

2.1 Materials characterization

It can be seen from Fig.1 that XRD pattern consists of one broad diffuse peak between diffraction angles 30° and 45°. It indicates that the specimen has perfect glassy structure. Besides, Fig.1 exhibits the DSC curve of specimen with a heating rate of 20 K/min. The glass transition temperature (T_g), onset crystallization temperature (T_x), melting temperature (T_m), supercooled liquid region ΔT_x ($\Delta T_x=T_x-T_g$) and parameter γ ($\gamma=T_x/(T_g+T_l)$) are summarized in Table 1. It can be seen from the DSC curve that there is obvious glass transition and crystallization process, which demonstrates glassy structure characteristics of the specimen again.

2.2 EDS analysis

The specimen was subjected to elemental quantitative analysis by EDS, and the uniformity of components was detected by surface scanning (Fig.2). The test results display that the internal chemical composition of the prepared specimen is distributed evenly. The mass fraction of alloy components is Zr (68.75 wt%), Cu (13.25 wt%), Ni (9.25 wt%), Al (3.24 wt%) and Er (5.52 wt%). The mass fraction calculated from the atomic fraction of alloy components is Zr (71.65 wt%), Cu (11.44 wt%), Ni (7.37 wt%), Al (4.01 wt%), and Er (5.53 wt%). Due to an error of about 3% of EDS, the component content of specimen meets the requirements of the nominal composition.

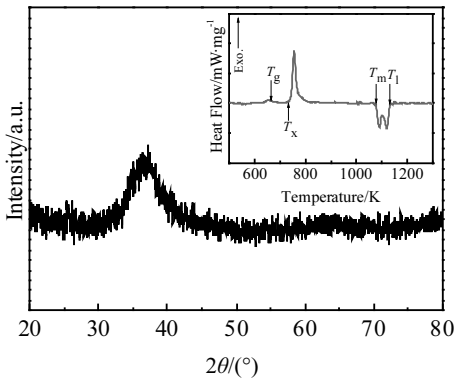

Fig.1 XRD pattern and DSC curve of the as-cast specimen

Table 1 Thermodynamic characteristic temperatures of specimen

T_g/K	T_x/K	T_m/K	T_l/K	ΔT_x/K	T_{rg}	γ
660	744	1081	1130	84	0.584	0.416

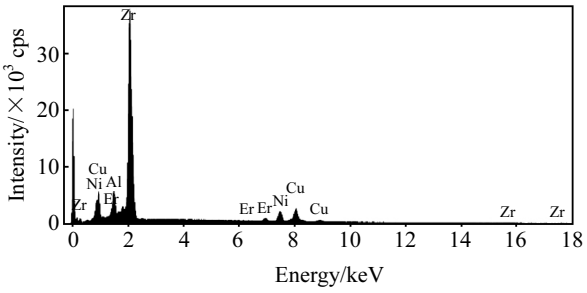

Fig.2 EDS spectrum of specimen

2.3 Effect of loading rate

Fig.3a represents the typical load (P)-displacement (h) curves of specimens at diverse loading rates with a load limit of 10,000 μN and a holding time of 10 s. The loading rates are 500, 1000, 1500 and 2000 μN/s. In order to make curves legible, each curve has been offset along the x-axis. It can be observed that there are creep platforms on each curve and the width of creep platform increases with the increase of loading rate. This phenomenon indicates that $(Zr_{0.6336}Cu_{0.1452}Ni_{0.1012}$-$Al_{0.12})_{97.4}Er_{2.6}$ BMG can undergo creep deformation at room temperature and its creep resistance at a lower loading rate is superior to that at a higher one. It can be seen from the unloading curve that the elastic recovery phenomenon occurs during the unloading process.

The creep displacement curves during holding period are

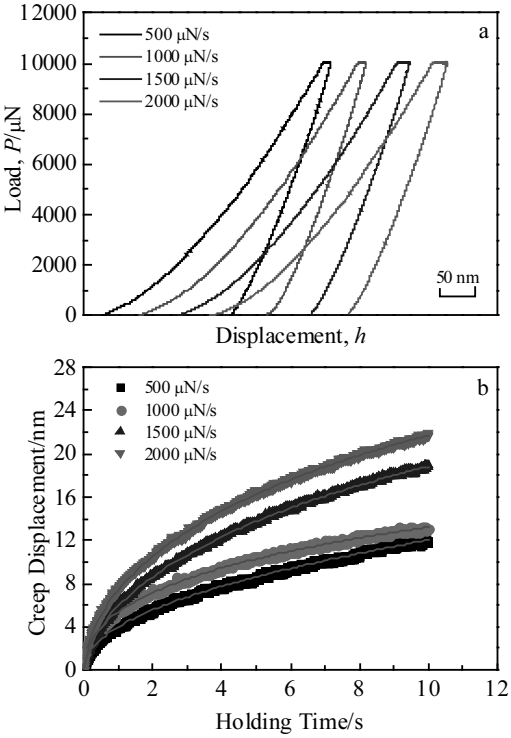

Fig.3 *P-h* curves (a) and creep displacement curves (b) at diverse loading rates

demonstrated in Fig.3b. For ease of comparison, the starting point of creep displacement is unified. It can be seen that the displacement of indenter increases rapidly with the increase of holding time in the early stage of holding period (transient creep), then the displacement rate becomes slower and changes with the holding time linearly (steady-state creep). Furthermore, it can be observed that the creep displacement climbs with the rise of loading rate, and the creep displacement exhibits strong loading rate dependence. The creep displacement ranges from 11.8 nm (appears at 500 μN/s) to 21.6 nm (appears at 2000 μN/s), as described in Fig.3b. Based on free volume theory, Hey et al [22] confirmed that the generation rate of free volume in the deformation is proportional to strain rate directly. Therefore, the faster the loading rate, the more the residual free volume is produced. Since the viscosity is proportional to the concentration of free volume inversely, the specimen may exhibit more macroscopic viscous flow behavior at high loading rate, resulting in occurrences of more creep displacement.

In addition, linear fitting was carried out on the curve of creep displacement-holding time in the stage of steady-state creep, in order to obtain steady-state creep rate of specimen. When the loading rate is 500, 1000, 1500 and 2000 μN/s, the corresponding steady-state creep rate is 0.6, 0.72, 1.08 and 1.12 nm/s, respectively. It grows with the increase of loading rate. This phenomenon may be due to the larger loading rate, which results in a larger free volume concentration. The larger free volume concentration makes the internal atomic rearrangement easier; therefore, the steady- state creep rate is faster.

The *P-h* curves of specimens can also provide a multitude of information. As described in Fig.4, the hardness (*H*) and elastic modulus (*E*) of specimens are calculated and their relationship with the loading rate is plotted. The *H* of each point was calculated at the peak load based on the Oliver-Pharr[23] method. *E* was calculated at the initial stage of unloading curve. When the loading rate is increased from 500 μN/s to 2000 μN/s, *H* decreases from 4.78 GPa to 4.35 GPa. Owing to the amount of free volume increasing with the increases of loading rate, a large loading rate means a large free volume concentration. The enrichment of free volume can reduce the *H* of specimen. It can be seen from Fig. 4 that the *E* drops with the rise of loading rate slightly. However, as a whole, the loading rate has little effect on *E*. When the loading rate is 500 μN/s, specimens have excellent mechanical properties, the minimal creep displacement is 11.8 nm, the maximum *H* is 4.78 GPa and the *E* is 54.66 GPa.

Fig.5 exhibits the *P-h* curves and a partially enlarged view at the loading period with different loading rates. It can be clearly seen that there is an obvious serrated flow phenomenon and this phenomenon differs at different loading rates. With the increases of loading rate, the serrated flow phenomenon decreases gradually. Specimen shows a significant serrated flow phenomenon, when the loading rate is 500 μN/s. However, when the loading rate is 2000 μN/s, few serrated flow phenomenon is observed.

There are two different explanations for the influence of loading rate on the serrated flow phenomenon. One is based on the lack of equipment accuracy and response time. It is considered that the equipment cannot observe small and discrete serrated flow phenomenon. The other explanation is that BMG undergoes essential transformation during the process of plastic deformation. At a lower rate, a single shear

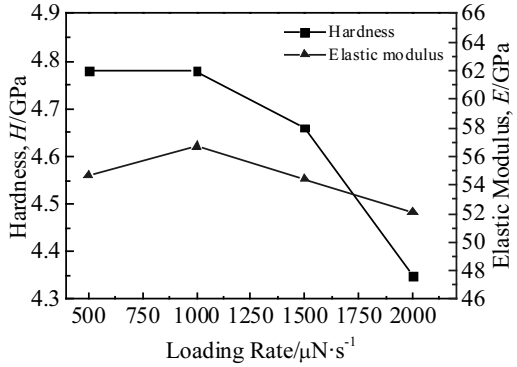

Fig.4 Relationship of hardness and elastic modulus with loading rate

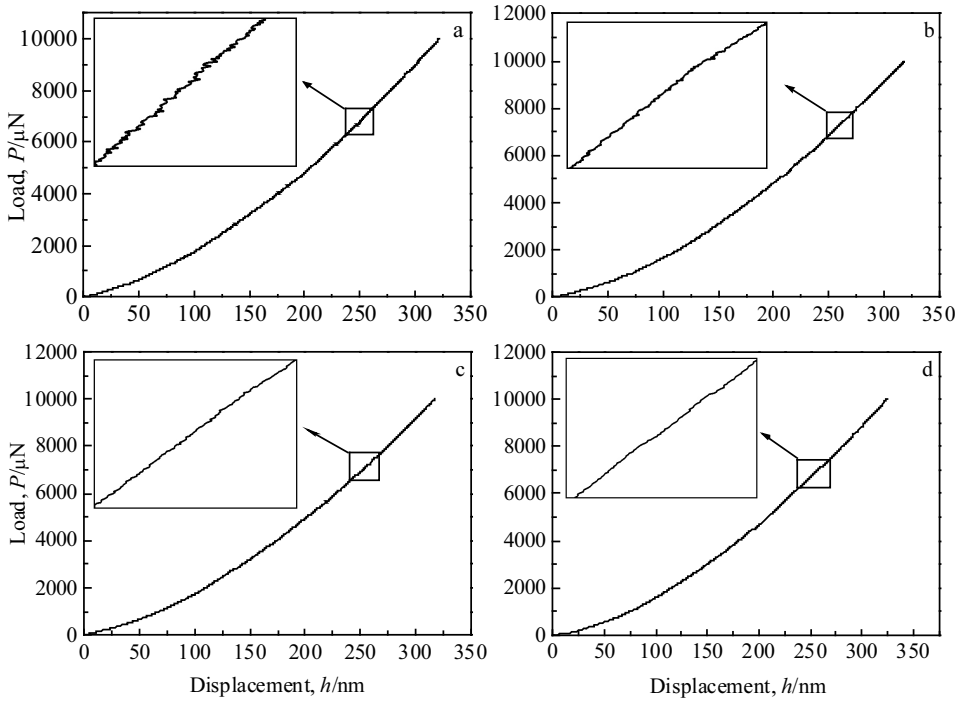

Fig.5 Load-displacement curves of specimen at loading stage with different loading rates: (a) 500 μN/s, (b) 1000 μN/s, (c) 1500 μN/s, and (d) 2000 μN/s

band can be fully extended to coordinate strain. At a higher rate, a single shear band cannot coordinate strain, thereby promoting the extending of multiple shear bands. The present work prefers the second explanation because it can be applied to the serrated flow phenomenon associated with the loading rate during the compression experiment at room temperature.

For a self-similar indentation tip like Berkovich tips, the strain rate $\dot{\varepsilon}$ and characteristic stress σ can be described as[24]:

$$\sigma = \frac{P}{24.56h^2} \tag{1}$$

$$\dot{\varepsilon} = \frac{1}{\mathrm{h}}\frac{\mathrm{d}h}{\mathrm{d}t} = \frac{\dot{h}}{h} \tag{2}$$

where P is the instantaneous load, $\dot{h}$ is the displacement rate of the tip of the Berkovich indenter, and h is the instantaneous displacement. The $\dot{h}$ has often been calculated by fitting the creep displacement curves according to the following empirical law[25]

$$h(t) = h_0 + a(t - t_0)^b + kt \tag{3}$$

where h_0 is the initial displacement depth; t_0 is the initial time of creep process; a, b and k are fitting parameters. The fitting parameters are shown in Table 2. Fig.3b demonstrates the relationship among the experimental creep data, the fitting data and holding time. It can be seen that the experimental curve fits well with the fitting curve. As can be seen from Table 2, the fitting degree (R^2) reaches 0.99. It is demonstrated that Eq. (3) can well describe the relationship between creep displacement and holding time of specimen. According to Eq. (2), the creep strain rate of specimen is calculated and the relationship between strain rate and holding time is plotted (Fig.6a).

Table 2 Fitting parameters of the fitted equation over creep displacement-time data

Fitting parameter	500 μN/s	1000 μN/s	1500 μN/s	2000 μN/s
h_0/nm	321.457 3	318.405 6	317.142 5	324.170 5
t_0/s	20.024 2	10.014 61	6.681 41	5.009 81
a	4.060 77	5.726 35	7.384 43	9.118 22
b	0.473 14	0.406 76	0.471 78	0.451 84
k	–0.002 49	–0.117 6	–0.177 85	–0.266 68
R^2	0.997 3	0.9975 1	0.999 12	0.999 19

Fig.6a demonstrates the relationship between creep strain rate and holding time of specimens at various loading rates. It can be seen that the creep strain rate decreases rapidly with the increase of holding time at the initial stage of creep (t<2s), and then slows down gradually and stabilizes eventually (t>2s). Moreover, the creep strain rates grow with the rise of loading rate. Fig.6b shows the relationship of the maximum depth of indentation and creep displacement with loading rate. The maximum depth is 347 nm which appears at 2000 μN/s and the minimum depth is 331 nm which appears at 500 μN/s. During the experiment, the maximum depth and creep

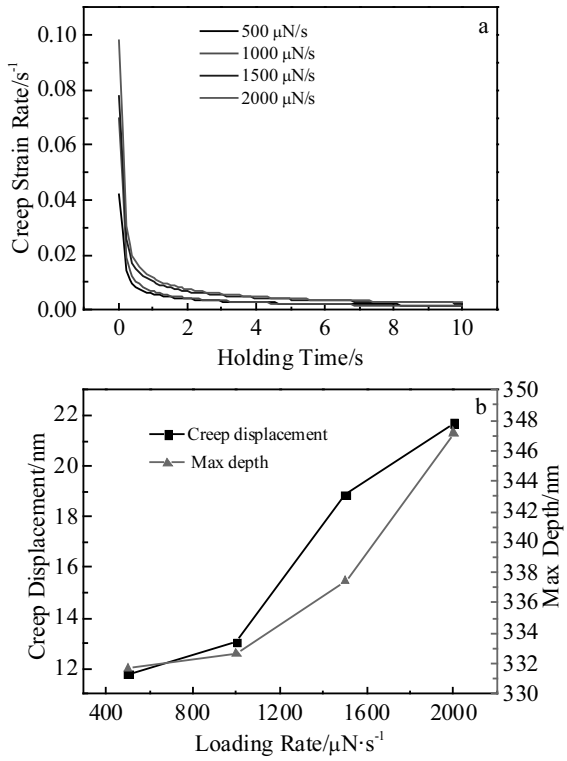

Fig.6 Relationship between strain rate and holding time of specimens (a); relationship of the max depth and creep displacement with loading rate (b)

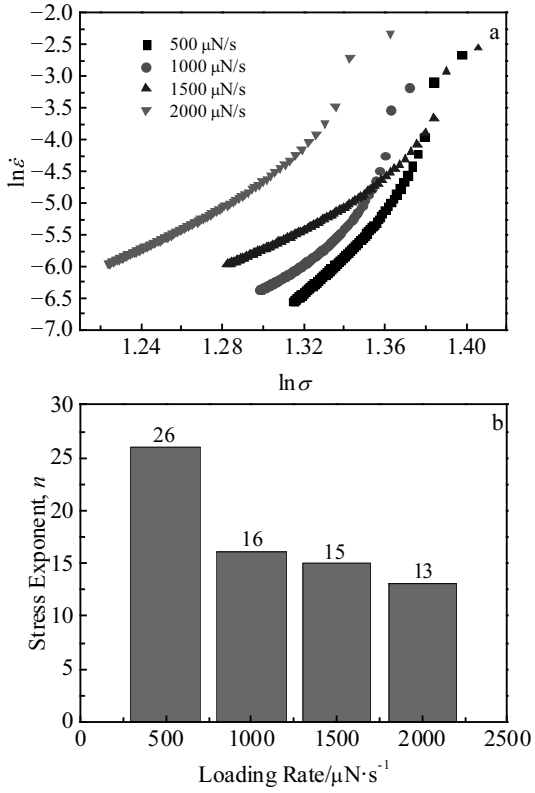

Fig.7 ln $\dot{\varepsilon}$ vs lnσ plots of specimen (a); relationship between creep stress exponent and loading rate (b)

displacement of indentation climb gradually with the rise of the loading rate. Fig.4 shows that the H of specimen decreases as the loading rate increases. Considering the conclusions of Fig.4 and Fig.6b, it can be concluded that the H of specimen drops with the growth of indentation depth. In other words, there is a size effect in the process of nanoindentation.

The relationship between strain rate $\dot{\varepsilon}$ and characteristic stress σ can be described by the classical power law equation[26]:

$$\dot{\varepsilon} = A\sigma^n \tag{4}$$

where the factor A is a temperature-dependent material constant. The creep stress exponent (n) is widely used to describe the steady-state creep behavior of material, because it can provide useful information about creep deformation. It can be described as:

$$n = \frac{\partial \ln\dot{\varepsilon}}{\partial \ln\sigma} \tag{5}$$

Fig.7a shows the ln $\dot{\varepsilon}$ vs lnσ curves under various loading rates. The n is taken from the slope of linear part of strain rate vs stress (corresponding to the very left region of the curve) and the relationship between n and loading rate is plotted as shown in Fig.7b. Fig.7b shows higher stress exponent values of 26 at 500 μN/s. The n exhibits strong loading rate dependence. With the rise of loading rate from 500 to 2000 μN/s, the n drops from 26 to 13. Similar behavior was observed by Huang et al[21]. A higher creep stress exponent means a stronger creep resistance. The experimental results shown in Fig.7b indicate that the specimen exhibits strong creep resistance at low loading rates.

The plastic deformation of BMG is usually described by its internal "flow defects", which can be clarified by free volume model. The change of free volume manifests density fluctuations, when the volume is greater than the critical volume v^*. The concentration of free volume c_f inside the BMG can be described as[27]:

$$c_f = \exp(-\frac{\gamma v^*}{v_f}) \tag{6}$$

where γ is a constant between 0.5 and 1; v_f is the average free volume of atoms. When an external stress is applied to the specimen, it undergoes a strain ε in the smaller region v_0, and the strain rate depends on the magnitude of applied stress. The macroscopic strain rate can be described by the following formula[28]:

$$\dot{\varepsilon}_u = 2c_f k_f \frac{\varepsilon_0 v_0}{\Omega} \sinh(\frac{\sigma\varepsilon_0 v_0}{2kT}) \tag{7}$$

where k represents Boltzmann's constant; T is temperature; k_f is a rate constant; Ω represents the atomic volume.

Ignoring the effect of temperature, in the nanoindentation

test, the creep strain rate is related to the macroscopic strain rate[29,30]. So the relationship between the creep strain rate and the c_f can be described as:

$$\dot{\varepsilon} = 0.18Bc_f \quad (8)$$

where B is a temperature-dependent material constant. Therefore, during the nanoindentation test, the concentration of free volume is correlated with the indentation strain rate positively. In addition, because plastic deformation of BMG depends on the generation and disappearance of free volume, the faster the indentation strain rate is before the creep stage, the more the viscous rheological behavior will exhibit. Therefore, the faster loading rate means more creep displacement. This conclusion is consistent with the experimental results which are shown in Fig.3 and Fig.7.

2.4 Effect of holding time

Fig.8a demonstrates *P-h* curves for diverse holding time at a load limit of 10 000 μN with a loading rate of 500 μN/s. The holding time is 5, 10, 15 and 20 s. It can be observed that the width of creep platform increases with the increase of holding time. This phenomenon indicates that creep displacement goes up with the growth of holding time. The plastic deformation of BMG is based on shear bands. Since the shearing phenomenon has a time effect, a longer holding time means more shear deformation, which further leads to more creep displacement. The relationship of creep displacement and max depth with holding time is shown in Fig.8b. It can be seen that the creep displacement range from 9 nm (appears at 5 s) to 23 nm (appears at 20 s). In addition, the max depth of indentation climbs with the increase of holding time. The H and E at different holding time are calculated according to Oliver-Pharr method, as shown in Fig.9a. The result shows that the H and E fall with the growth of holding time. It can be observed that the specimen has a size effect during nanoindentation process which is manifested by the fact that the H drops with the rise of indentation depth by comparing Fig.8b and Fig.9a. Ignoring the influence of temperature, plastic deformation caused by stress grows with the rise of holding time. The plastic deformation of BMG is based on shear band, and more shear bands mean more free volumes. The enrichment of free volume results in a decrease in H. Fig.9b shows the relationship between creep strain rate and holding time. It can be obtained that the creep deformation consists of transient creep and steady-state creep. The creep strain rate curves at different holding time almost coincide, indicating that the creep strain rate of specimen does not depend on holding time.

The $\ln\dot{\varepsilon}$ vs $\ln\sigma$ curves of specimen at different holding time are plotted as described in Eq.(5), as shown in Fig.10a. The slope of the curve decreases with the increase of holding time gradually and exhibits a tendency to vary linearly at the end of holding time. Fig.10b displays the relationship between creep stress exponents and holding time. The transient creep behavior of BMG is affected by elastic deformation, so the creep stress exponent is extracted from the end of holding

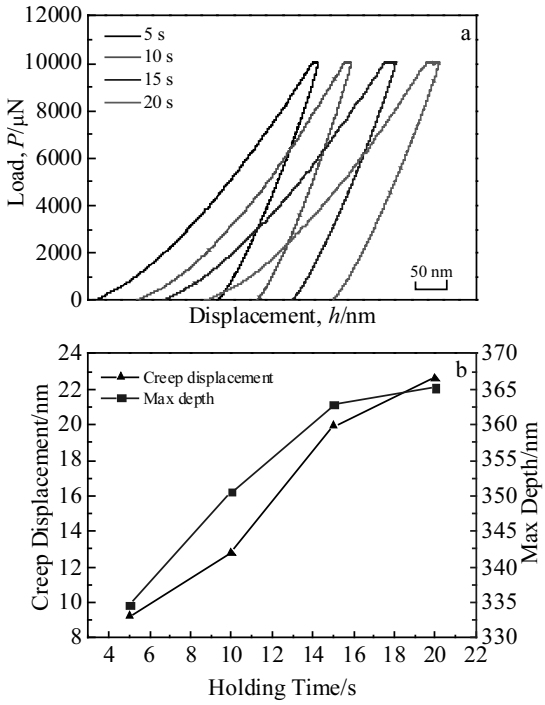

Fig.8 Load-displacement curves of specimen with diverse holding time (a); relationship among creep displacement, max depth and holding time (b)

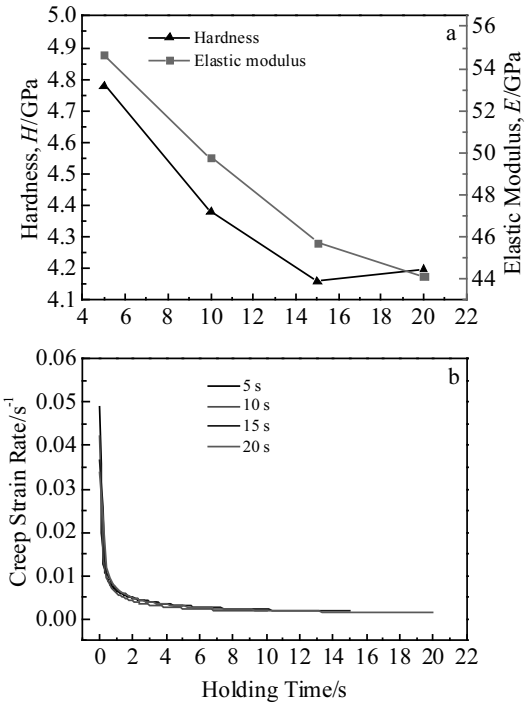

Fig.9 Relationship of hardness and elastic modulus with holding time (a); relationship between strain rate and holding time (b)

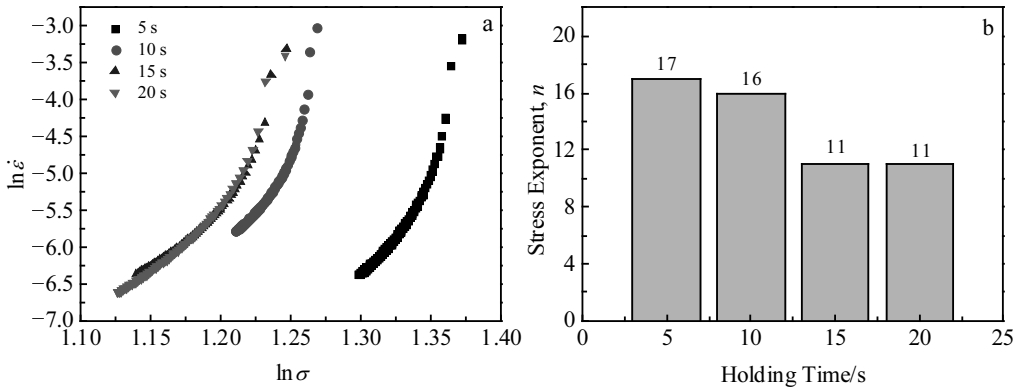

Fig.10 ln $\dot{\varepsilon}$ vs lnσ curves of specimen with diverse holding time (a); relationship between creep stress exponent and holding time (b)

time in the present work. The stress exponent drops with the growth of holding time (Fig.10b). It indicates that the creep resistance decreases with the increase of holding time. Due to the time dependence of shearing phenomenon, a long holding time affects shear deformation, resulting in an increase of creep displacement and a decrease of the creep stress exponent. When the holding time reaches 15 and 20 s, the creep stress exponents is consistent, indicating that the creep deformation of specimens tends to be stable.

Fig.11 displays the SPM images of indentation profile at different holding time. Specimens demonstrate distinct indentation profiles at different holding time. The surface of specimen indicates a shape of Berkovich indenter and a material pile up phenomenon. The material piles up in Fig.11c, 11d are more than that of Fig.11a, 11b. The reason for this phenomenon can be explained in two aspects. On the one hand, the longer holding time means the deeper indentation depth, resulting in more material piles up. On the other hand, the longer the holding time, the more significant the enrichment of free volume, and the H of specimen falls, which further lead to more material piles up.

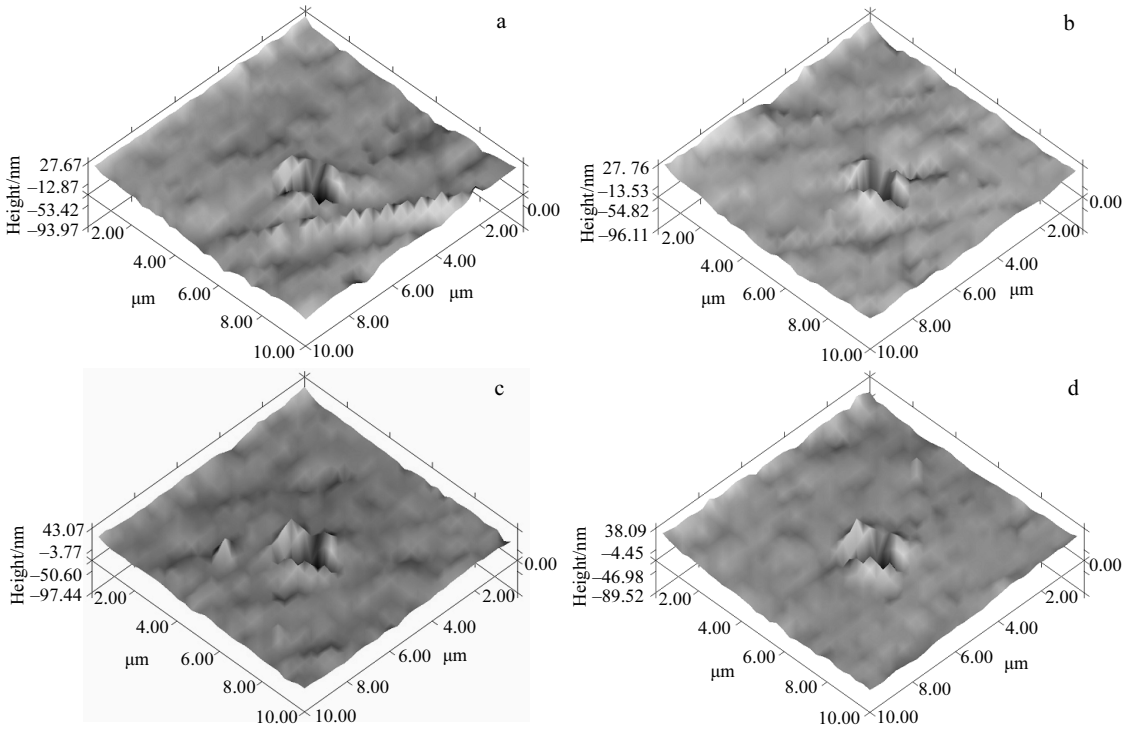

Fig.11 SPM images of the indentation topography of specimens at different holding time: (a) 5 s, (b) 10 s, (c) 15 s, and (d) 20 s

3 Conclusions

1) The creep displacement of $(Zr_{0.6336}Cu_{0.1452}Ni_{0.1012}Al_{0.12})_{97.4}Er_{2.6}$ BMG increases with the increase of loading rate or holding time.

2) The specimen has a size effect during nanoindentation process, and the *H* drops with the rise of indentation depth. The *H* also falls with the growth of loading rate or holding time.

3) The specimen has a serrated flow phenomenon during the nanoindentation process and has rate dependence. As the loading rate declines, the serrated flow phenomenon becomes more obvious.

4) The creep deformation process of specimen is mainly composed of two parts: one part is transient creep (t<2 s) and the other part is steady state creep (t>2 s). The creep strain rate of specimen climbs with the loading rate.

5) The creep stress exponent declines with the increases of loading rate or the holding time.

References

1 Hufnagel T C, Schuh C A, Falk M L. *Acta Materialia*[J], 2016, 109(4): 375

2 Inoue A, Shen B, Koshiba H *et al*. *Nature Materials*[J], 2003, 2(10): 661

3 Inoue A, Takeuchi A. *Acta Materialia*[J], 2011, 59(6): 2243

4 Kumar G, Neibecker P, Liu Y H *et al*. *Nature Communications*[J], 2013, 4: 1536

5 Schroers J. *Acta Materialia*[J], 2010, 22(14): 1566

6 Schuh C A, Hufnagel T C. *Acta Materialia*[J], 2007, 55(12): 4067

7 Nishiyama N, Takenaka K, Miura H *et al*. *Intermetallics*[J], 2012, 30: 19

8 Chen Y C, Chu J P, Jang J S C *et al*. *Materials Science & Engineering A*[J], 2012, 556: 488

9 Long Z, Shao Y, Xie G *et al*. *Journal of Alloys and Compounds*[J], 2008, 462(1-2): 52

10 Babu P S, Jha R, Guzman M *et al*. *Materials Science and Engineering A*[J], 2016, 658: 415

11 Castellero A, Moser B, Uhlenhaut D I *et al*. *Acta Materialia*[J], 2008, 56(15): 3777

12 Ma Y, Peng G J, Feng Y H *et al*. *Journal of Non-Crystalline Solids*[J], 2017, 465: 8

13 Schuh C A, Nieh T G. *Acta Materialia*[J], 2003, 51(1): 87

14 Xu F, Zeng N, Cheng K *et al*. *Journal of Non-Crystalline Solids* [J], 2018, 490: 50

15 Yoo B G, Choi I C, Kim Y J *et al*. *Materials Science and Engineering A*[J], 2013, 577: 101

16 Yoo B G, Oh J H, Kim Y J *et al*. *Intermetallics*[J], 2010, 18(10): 1898

17 Yu P F, Feng S D, Xu G S *et al*. *Scripta Materialia*[J], 2014, 90-91: 45

18 Wang X, Gong P, Deng L *et al*. *Journal of Non-Crystalline Solids*[J], 2017, 470(15): 27

19 Zhang T H, Ye J H, Feng Y H *et al*. *Materials Science & Engineering A*[J], 2017, 685: 294

20 Huang Y J, Chiu Y L, Shen J *et al*. *Journal of Materials Research*[J], 2009, 24(3): 993

21 Huang Y J, Shen J, Chiu Y L *et al*. *Intermetallics*[J], 2009, 17(4): 190

22 Hey P D, Sietsma J, Beukel A V D. *Acta Materialia*[J], 1998, 46(16): 5873

23 Oliver W C, Pharr G M. *Journal of Materials Research*[J], 1992, 7(6): 1564

24 Lucas B N, Oliver W C. *Metallurgical and Materials Transactions A*[J], 1999, 30(3): 601

25 Li H, Ngan A H W. *Journal of Materials Research*[J], 2004, 19(2): 513

26 Goodall R, Clyne T W. *Acta Materialia*[J], 2006, 54(20): 5489

27 Spaepen F. *Acta Metallurgica*[J], 1977, 25(4): 407

28 Xu F, Long Z L, Deng X H *et al*. *Transactions of Nonferrous Metals Society of China*[J], 2013, 23(6): 1646

29 Schuh C A, Nieh T G. *Acta Materialia*[J], 2003, 51(1): 87

30 Kim J J, Choi Y, Suresh S *et al*. *Science*[J], 2002, 295(5555): 654

Zr 基块体金属玻璃蠕变行为的纳米压痕研究

李春燕[1,2]，朱福平[1]，丁娟强[1]，尹金锋[1]，王　铮[3]，赵燕春[1,2]，寇生中[1,2]

(1. 兰州理工大学 省部共建有色金属先进加工与再利用国家重点实验室，甘肃 兰州 730050)

(2. 兰州理工大学 温州泵阀工程研究院，浙江 温州 325105)

(3. 中国重汽集团济南卡车有限公司，山东 济南 250000)

摘　要：通过纳米压痕实验研究了加载速率和保载时间对$(Zr_{0.6336}Cu_{0.1452}Ni_{0.1012}Al_{0.12})_{97.4}Er_{2.6}$块体金属玻璃（BMG）的蠕变变形行为的影响。实验结果表明，合金试样的蠕变位移随着加载速率或保载时间的增加而增大。另一方面，合金样品的硬度（*H*）也随着加载速率或保载时间的增加而降低。合金试样在纳米压痕过程中具有尺寸效应，合金试样的硬度随着压痕深度的增加而降低。合金试样在纳米压痕过程中具有锯齿流动现象，并且该现象具有速率依赖性。具体而言，随着加载速率的减小，锯齿流动现象更加明显。合金试样的蠕变应力指数随着加载速率或保载时间的增加而减小。

关键词：纳米压痕；硬度；加载速率；应力指数；保载时间

作者简介：李春燕，女，1979 年生，博士，教授，兰州理工大学材料科学与工程学院，甘肃 兰州 730050，电话：0931-2976378，E-mail: licywz@163.com